

# SOFT X-RAY EXTENDED EMISSIONS OF SHORT GAMMA-RAY BURSTS AS ELECTROMAGNETIC COUNTERPARTS OF COMPACT BINARY MERGERS; POSSIBLE ORIGIN AND DETECTABILITY

TAKASHI NAKAMURA<sup>1</sup>, KAZUMI KASHIYAMA<sup>2</sup>, DAISUKE NAKAUCHI<sup>1</sup>, YUDAI SUWA<sup>3</sup>,  
TAKANORI SAKAMOTO<sup>4</sup>, AND NOBUYUKI KAWAI<sup>5</sup>

*Draft version November 23, 2018*

## ABSTRACT

We investigate the possible origin of extended emissions (EE) of short gamma-ray bursts (SGRBs) with an isotropic energy of  $\sim 10^{50-51}$  erg and a duration of  $\sim 100$  s, based on the compact binary (neutron star (NS)-NS or NS-black hole (BH)) merger scenario. We analyze the evolution of magnetized neutrino-dominated accretion disks of mass  $\sim 0.1 M_{\odot}$  around BHs formed after the mergers, and estimate the power of relativistic outflows via the Blandford-Znajek (BZ) process. We show that a rotation energy of the BH up to  $\sim 10^{53}$  erg can be extracted with a time scale of  $\sim 100$  s with a disk viscosity parameter of  $\alpha \sim 0.01$ . Such a BZ power dissipates by clashing with non-relativistic pre-ejected matter of mass  $M \sim 10^{-(2-4)} M_{\odot}$ , and form a mildly relativistic fireball. We show that the dissipative photospheric emissions from such fireballs are likely in soft X-ray band (1-10 keV) for  $M \sim 10^{-2} M_{\odot}$  possibly in NS-NS mergers, and in the BAT band (15-150 keV) for  $M \sim 10^{-4} M_{\odot}$  possibly in NS-BH mergers. In the former case, such soft EEs can provide a good chance of  $\sim 6 \text{ yr}^{-1}$  ( $\Delta\Omega_{\text{softEE}}/4\pi$ ) ( $\mathcal{R}_{\text{GW}}/40 \text{ yr}^{-1}$ ) for simultaneous detections of the gravitational waves with a  $\sim 0.1^{\circ}$  angular resolution by soft X-ray survey facilities like Wide-Field MAXI. Here,  $\Delta\Omega_{\text{softEE}}$  is the beaming factor of the soft EEs and  $\mathcal{R}_{\text{GW}}$  is the NS-NS merger rate detectable by advanced LIGO, advanced Virgo, and KAGRA. While in the latter case, the observed EEs, which are associated with  $\sim 25\%$  of *Swift* SGRBs, can be well explained although the simultaneous detection rate with the GWs is expected to be very low  $\lesssim 10^{-3} \text{ yr}^{-1}$ .

*Subject headings:* gamma rays: bursts — gamma rays: observations — gamma rays: theory

## 1. INTRODUCTION

Short gamma-ray bursts (SGRBs) are usually defined by the prompt duration, i.e., GRBs with  $T_{90} < 2$  s (Kouveliotou et al. 1993). A significant fraction of the SGRBs are accompanied by longer duration ( $\sim 100$  s) extended emissions (EEs). The isotropic energy of prompt spike is  $E_{\text{iso},PS} \sim 10^{50-51}$  erg (Tsutsui et al. 2013), while that of EE is  $E_{\text{iso},EE} \sim 10^{50-51}$  erg (Sakamoto et al. 2011). Interestingly, in some cases, observed fluences of the EEs are even larger than those of the prompt spikes, e.g.,  $E_{\text{iso},EE} \sim 2.7 \times E_{\text{iso},PS}$  for SGRB 050709 (Villasenor et al. 2005) and  $E_{\text{iso},EE} \sim 30 \times E_{\text{iso},PS}$  for SGRB 080503 (Perley et al. 2009). Fong et al. (2013) found that  $\sim 25\%$  of *Swift* BAT SGRBs have EEs in the X-ray band (see their Table. 3). On the other hand, Bostanci et al. (2013) searched EEs in 296 BATSE SGRBs and found that the fraction of EE is  $\sim 7\%$ , where they pointed out that this fraction should be regarded as the minimum value since dim and/or softer EEs cannot be detected by BATSE. In fact, BATSE measured flu-

ence above 20 keV while BAT does down to 15 keV, and the 5 keV lower threshold energy yields 18% increase of the EE population. This suggests that the decrease of the threshold energy, say, as low as  $\sim 1$  keV, might yield the dramatic increase of the EE population.

Here, we consider the possible origin of such EEs based on the compact binary (neutron star (NS)-NS or NS-black hole (BH)) merger scenario (Paczynski 1986; Goodman 1986; Eichler et al. 1989; Narayan et al. 1992). If the maximum mass of non-rotating NS is smaller than  $\sim 2.5 M_{\odot}$ , the final outcome of such a merger will be a Kerr black hole (BH) of mass  $M_{\text{BH}} \sim 3 M_{\odot}$  and spin parameter  $q = a/M_{\text{BH}} < 0.8$  with an accretion disk of mass  $\sim 0.1 M_{\odot}$  and a neutron-rich ejecta of mass  $M \sim 10^{-(2-4)} M_{\odot}$  with an expanding velocity of  $v_{\text{exp}} \sim 0.1c$  (Shibata & Taniguchi 2006; Kiuchi et al. 2009; Rezzolla et al. 2010; Hotokezaka et al. 2011, 2013). Here, we adopt this situation, while if the maximum mass of non-rotating NS is larger than  $\sim 2.5 M_{\odot}$ , a rapidly rotating massive NS will be the final outcome, and the magnetar activities may be responsible for the prompt spike and EE of SGRBs, and also other electromagnetic counterparts (Usov 1992; Zhang & Mészáros 2001; Gao & Fan 2006; Metzger et al. 2008; Bucciantini et al. 2012; Gompertz et al. 2013; Zhang 2013).

In this paper, we consider the huge rotational energy of the Kerr BH as the intrinsic energy budget of the EE. The mass formula of the Kerr BH with the gravitational mass  $M_{\text{BH}}$  and the angular momentum  $J$  is written as

<sup>1</sup> Department of Physics, Kyoto University, Oiwake-cho, Kitashirakawa, Sakyo-ku, Kyoto 606-8502, Japan

<sup>2</sup> Department of Astronomy & Astrophysics; Department of Physics; Center for Particle & Gravitational Astrophysics; Pennsylvania State University, University Park, PA 16802

<sup>3</sup> Yukawa Institute for Theoretical Physics, Kyoto University, Oiwake-cho, Kitashirakawa, Sakyo-ku, Kyoto 606-8502, Japan

<sup>4</sup> Department of Physics and Mathematics, College of Science and Engineering, Aoyama Gakuin University, 5-10-1 Fuchinobe, Chuo-ku, Sagamihara-shi, Kanagawa 252-5258, Japan

<sup>5</sup> Department of Physics, Tokyo Institute of Technology, 2-12-1 Ookayama, Meguro-ku, Tokyo 152-8551, Japan

(Misner et al. 1973)

$$M_{BH}^2 = M_{ir}^2 + \frac{J^2}{4M_{ir}^2}, \quad (1)$$

where  $M_{ir}$  is the irreducible mass of Kerr BH. Writing  $J = aM_{BH} = qM_{BH}^2$ , we have

$$M_{BH}^2 = M_{ir}^2 + \frac{M^4 q^2}{4M_{ir}^2}, \quad (2)$$

where  $a$  is the well known Kerr parameter and  $q = a/M_{BH} < 1$ . Eq. (2) is rewritten as

$$M_{BH}^2 = \frac{2M_{ir}^2}{1 + \sqrt{1 - q^2}}. \quad (3)$$

Then, the available energy by the extraction of the angular momentum of the Kerr BH is given by

$$\Delta E = M_{BH} \left( 1 - \sqrt{\frac{1 + \sqrt{1 - q^2}}{2}} \right). \quad (4)$$

For  $q = 0.5$ , for example,  $\Delta E$  is given by

$$\Delta E = 1.84 \times 10^{53} \text{ erg} \left( \frac{M_{BH}}{3 M_\odot} \right). \quad (5)$$

Therefore, for an  $\sim 100\%$  radiation efficiency, only an  $\sim 1\%$  of the rotational energy of the BH enables to fuel an EE even if the emission is isotropic. The problem is how to extract the rotational energy of the Kerr BH in a time scale of  $\sim 100$  s.

One of the plausible mechanisms to extract the rotation energy of the Kerr BH is the Blandford-Znajek (BZ) process (Blandford & Znajek 1977). From the results of numerical simulations, Penna et al. (2013) found that within factors of order unity, the BZ power is expressed in the units of  $c = G = 1$  by

$$L^{BZ} = \frac{1}{6\pi} \Omega_H^2 \Phi^2, \quad (6)$$

where

$$\Omega_H = M_{BH}^{-1} \times \frac{q}{(1 + \sqrt{1 - q^2})^2 + q^2} \quad (7)$$

and

$$\Phi = \pi M_{BH}^2 (1 + \sqrt{1 - q^2})^2 B \quad (8)$$

is the magnetic flux threading the horizon with  $B$  being the strength of the magnetic field formed by the disk around the Kerr BH. Recovering  $c$  and  $G$ , we have

$$L^{BZ} = \frac{\pi}{6} \left[ \frac{q(1 + \sqrt{1 - q^2})^2}{(1 + \sqrt{1 - q^2})^2 + q^2} \right]^2 \left( \frac{GM_{BH}}{c^2} \right)^2 cB^2. \quad (9)$$

For  $q = 0.5$ , for example,  $L^{BZ}$  is expressed as

$$L^{BZ} = 6.6 \times 10^{50} \text{ erg s}^{-1} \left( \frac{M_{BH}}{3 M_\odot} \right)^2 \left( \frac{B}{10^{15} \text{ G}} \right)^2. \quad (10)$$

Dividing Eq. (5) with Eq. (10) we have the characteristic time  $\delta t_{BZ}$  as

$$\delta t_{BZ} = 2.8 \times 10^2 \text{ s} \left( \frac{M_{BH}}{3 M_\odot} \right)^{-1} \left( \frac{B}{10^{15} \text{ G}} \right)^{-2}. \quad (11)$$

This shows that if the accretion disk with  $B \sim 10^{15} \text{ G}$  and an accretion time  $\sim 100$  s exists, up to  $\sim 10^{53} \text{ erg}$  can be extracted from the Kerr BH. This is just the time scale of the EE and only  $\sim 1\%$  efficiency is enough to explain them even if they are isotropic emissions.

This paper is organized as follows. In §2, we analyze the time evolution of the neutrino-dominated accretion disk with finite mass and angular momentum around the BH, and estimate the resultant BZ power and the duration. In §3, we consider the interaction of the BZ jets with the pre-ejected matter ( $M \sim 10^{-(2-4)} M_\odot$ ) with the expanding velocity of  $v_{exp} \sim 0.1c$ , which produce mildly relativistic fireballs. We calculate the dissipative photospheric emissions from such fireballs. There, we also argue the detectability and the association with the observed EEs. §4 is devoted to discussions. We use  $Q_x = Q/10^x$  in CGS units unless otherwise noted.

## 2. BLANDFORD-ZNAJEK JETS FROM BLACK-HOLE TORI FORMED AFTER COMPACT BINARY MERGERS

Chen & Beloborodov (2007) performed the detailed numerical simulations of the neutrino-dominated accretion disk around the Kerr BH, which is also the case in our setup at the initial stage. They assumed the accretion rate  $\dot{M}(t) = \text{constant}$ , but took into account the full neutrino process and the Kerr geometry. Their important conclusions are that (i) the pressure is dominated by baryons with  $p = (\rho/m_p)kT$ , (ii) the disk is neutron dominated so that the electron fraction is as small as  $Y_e \sim 0.1$ , (iii) the degeneracy of the electron is at most mild because, if the degeneracy is high, the neutrino cooling is lowered to increase the temperature, (iv) there is an ignition accretion rate for neutrino cooling disk which is proportional to  $\alpha^{5/3}$  where  $\alpha$  is the parameter in the so-called  $\alpha$ -disk model (Shakura & Sunyaev 1973). Kawanaka et al. (2013) performed the simpler Newtonian calculations of such disks both numerically and analytically. One of the important conclusions are that their analytical model fits well with the numerical ones by Chen & Beloborodov (2007). Therefore, here we adopt a simple Newtonian analytical model to mimic the neutrino-dominated accretion disk around the Kerr BH. One of the big difference from Kawanaka et al. (2013) is that we take into account the time variation of the accretion rate for the finite disk mass and the finite disk angular momentum while they considered the constant accretion rate.

The structure of the accretion disk can be derived from (Kawanaka et al. 2013)

$$\dot{M} = -2\pi r \times 2\rho h v_r, \quad (12)$$

$$2\alpha h p = \frac{\dot{M} \Omega}{2\pi}, \quad (13)$$

$$p = \rho \Omega^2 h^2, \quad (14)$$

where  $\dot{M}$ ,  $r$ ,  $\rho$ ,  $h$ ,  $v_r$ ,  $\alpha$ ,  $p$  and  $\Omega$  are the accretion rate,  $r$  in the cylindrical coordinate, the density, the half thickness of the disk, the in falling velocity,  $\alpha$  parameter, the pressure and the angular frequency of the disk, respectively.

We can express  $h, p, v_r$  by  $\rho$  as

$$\begin{aligned}
h &= \left( \frac{\dot{M}}{4\pi\alpha\Omega\rho} \right)^{1/3} \\
&= 7.02 \times 10^8 \text{ cm } \alpha_{-1}^{-1/3} \rho_0^{-1/3}, \\
&\quad \times \left( \frac{\dot{M}}{10^{-3}M_\odot s^{-1}} \right)^{1/3} \left( \frac{M_{BH}}{3 M_\odot} \right)^{1/3} \left( \frac{r}{r_{ISCO}} \right)^{1/2} \quad (15) \\
p &= \Omega^{4/3} \rho^{1/3} \left( \frac{\dot{M}}{4\pi\alpha} \right)^{2/3} \\
&= 1.04 \times 10^{25} \text{ dyn cm}^{-2} \alpha_{-1}^{-2/3} \rho_0^{1/3}, \\
&\quad \times \left( \frac{\dot{M}}{10^{-3}M_\odot s^{-1}} \right)^{2/3} \left( \frac{M_{BH}}{3 M_\odot} \right)^{-4/3} \left( \frac{r}{r_{ISCO}} \right)^{-2} \quad (16) \\
v_r &= - \left( \frac{\dot{M}}{4\pi\rho} \right)^{2/3} (\alpha\Omega)^{1/3} \frac{1}{r} \\
&= -8.49 \times 10^{13} \text{ cm s}^{-1} \alpha_{-1}^{1/3} \rho_0^{-2/3}, \\
&\quad \times \left( \frac{\dot{M}}{10^{-3}M_\odot s^{-1}} \right)^{2/3} \left( \frac{M_{BH}}{3 M_\odot} \right)^{-4/3} \left( \frac{r}{r_{ISCO}} \right)^{-3/2} \quad (17)
\end{aligned}$$

where

$$r_{ISCO} = 6GM_{BH}/c^2, \quad (18)$$

is the innermost stable circular orbit (ISCO).<sup>6</sup> The density  $\rho$  can be determined by the energy equation and the equation of state. Denoting the cooling rate  $\dot{q}$ , the energy balance is expressed as

$$\begin{aligned}
\dot{q} &= \frac{3GM_{BH}\dot{M}}{4\pi r^3 \times 2h} \\
&= 7.16 \times 10^{27} \text{ erg cm}^{-3} \text{ s}^{-1} \alpha_{-1}^{1/3} \rho_0^{1/3} \\
&\quad \times \left( \frac{\dot{M}}{10^{-3}M_\odot s^{-1}} \right)^{2/3} \left( \frac{M_{BH}}{3 M_\odot} \right)^{-7/3} \left( \frac{r}{r_{ISCO}} \right)^{-7/2} \quad (20)
\end{aligned}$$

As for the energy loss rate, we consider two neutrino cooling processes relevant to the accretion disk we are interested in as (Itoh et al. 1989; Popham et al. 1999)

$$\dot{q}_{URCA} = 9 \times 10^{-43} \text{ erg cm}^{-3} \text{ s}^{-1} \rho_0 T_0^6, \quad (21)$$

$$\dot{q}_{pair} = 5 \times 10^{-66} \text{ erg cm}^{-3} \text{ s}^{-1} T_0^9, \quad (22)$$

where  $T$  is the temperature in unit of [K]. The URCA process is  $p + e^- \rightarrow n + \nu_e, n + e^+ \rightarrow p + \bar{\nu}_e$  and pair neutrino process is  $e^- + e^+ \rightarrow \nu_e + \bar{\nu}_e$ . The URCA process dominates over pair process for  $\rho > 5.5 \times 10^{-24} T^3$ . As for the pressure of the matter we should consider

$$p = \frac{\rho k T}{m_p} \quad (\text{gas pressure}), \quad (23)$$

<sup>6</sup> In fact, the location of the ISCO depends on  $q = a/M$ . However we are using Newtonian gravity so that the exact treatment of ISCO is not possible. One can take into account the change of ISCO by putting different value of  $r/6GM_{BH}/c^2$  in all the equations. In this case, various quantities are modified by powers of the above factor, but our results do not change qualitatively.

$$p = \frac{1}{3} a_{rad} T^4 \quad (\text{pressure by radiation}), \quad (24)$$

$$p = \frac{2\pi ch}{3} \left( \frac{3Y_e \rho}{8\pi m_p} \right)^{4/3} \quad (\text{degenerate electron}), \quad (25)$$

where  $a_{rad} = 7.57 \times 10^{-15} \text{ erg cm}^{-3} \text{ K}^{-4}$  is the radiation constant. The relativistically degenerate pressure dominates over the gas and the radiation pressure for  $\rho > 2.3 \times 10^{-22} \text{ g cm}^{-3} (Y_e/0.5)^{-4} T_0^3$  while the gas pressure dominates over the radiation pressure for  $\rho > 3.06 \times 10^{-23} \text{ g cm}^{-3} T_0^3$

Let us consider the case for  $3.06 \times 10^{-23} T_0^3 < \rho_0 < 1.4 \times 10^{-19} T_0^3$ , then the pressure is determined by gas pressure, and the cooling process is dominated by URCA process so that Eqs. (20) and (21) give

$$\begin{aligned}
&7.18 \times 10^{27} \alpha_{-1}^{1/3} \rho_0^{1/3} \\
&\quad \times \left( \frac{\dot{M}}{10^{-3}M_\odot s^{-1}} \right)^{2/3} \left( \frac{M_{BH}}{3 M_\odot} \right)^{-7/3} \left( \frac{r}{r_{ISCO}} \right)^{-7/2} \\
&= 9 \times 10^{-43} \rho_0 T_0^6, \quad (26)
\end{aligned}$$

with  $p = \rho k T / m_p$ .

From Eqs. (16), (23), and (26),  $\rho$  is expressed as

$$\begin{aligned}
\rho &= 6.47 \times 10^9 \text{ g cm}^{-3} \alpha_{-1}^{-13/10} \\
&\quad \times \left( \frac{\dot{M}}{10^{-3}M_\odot s^{-1}} \right) \left( \frac{M_{BH}}{3 M_\odot} \right)^{-17/10} \left( \frac{r}{r_{ISCO}} \right)^{-51/20} \quad (27)
\end{aligned}$$

We have then

$$\begin{aligned}
h &= 3.77 \times 10^5 \text{ cm } \alpha_{-1}^{1/10} \\
&\quad \times \left( \frac{M_{BH}}{3 M_\odot} \right)^{9/10} \left( \frac{r}{r_{ISCO}} \right)^{27/20}, \quad (28)
\end{aligned}$$

$$\begin{aligned}
p &= 1.94 \times 10^{28} \text{ dyn cm}^{-2} \alpha_{-1}^{-11/10} \\
&\quad \times \left( \frac{\dot{M}}{10^{-3}M_\odot s^{-1}} \right) \left( \frac{M_{BH}}{3 M_\odot} \right)^{-19/10} \left( \frac{r}{r_{ISCO}} \right)^{-57/20} \quad (29)
\end{aligned}$$

$$T = 3.63 \times 10^{10} \text{ K } \alpha_{-1}^{1/5} \left( \frac{M_{BH}}{3 M_\odot} \right)^{-1/5} \left( \frac{r}{r_{ISCO}} \right)^{-3/10} \quad (30)$$

$$v_r = -2.45 \times 10^7 \text{ cm s}^{-1} \alpha_{-1}^{6/5} \left( \frac{M_{BH}}{3 M_\odot} \right)^{-1/5} \left( \frac{r}{r_{ISCO}} \right)^{1/5}, \quad (31)$$

$$\begin{aligned}
v_r/v_{kep} &= -2.00 \times 10^{-3} \alpha_{-1}^{6/5}, \\
&\quad \times \left( \frac{M_{BH}}{3 M_\odot} \right)^{-1/5} \left( \frac{r}{r_{ISCO}} \right)^{7/10}, \quad (32)
\end{aligned}$$

$$v_{kep} = 1.22 \times 10^{10} \text{ cm s}^{-1} \left( \frac{r}{r_{ISCO}} \right)^{-1/2}. \quad (33)$$

Then, the surface density of the disk ( $\Sigma$ ) is given by

$$\Sigma = 2\rho h = 4.88 \times 10^{15} \text{ g cm}^{-2} \alpha_{-1}^{-6/5} \times \left( \frac{\dot{M}}{10^{-3} M_{\odot} \text{ s}^{-1}} \right) \left( \frac{M_{BH}}{3 M_{\odot}} \right)^{-4/5} \left( \frac{r}{r_{ISCO}} \right)^{-6/5} \quad (34)$$

Let us introduce the coordinate  $x$  by  $r = x \times r_{ISCO}$ . We here assume that the disk has the minimum and the maximum  $x$  as  $x_{min} = 1$  and  $x_{max}$ , respectively. Then for a given total mass  $m_d$  and the total angular momentum  $J_t$ , we have

$$m_d = 1.36 \times 10^{-4} M_{\odot} \alpha_{-1}^{-6/5} (x_{max}^{4/5} - 1) \times \left( \frac{\dot{M}}{10^{-3} M_{\odot} \text{ s}^{-1}} \right) \left( \frac{M_{BH}}{3 M_{\odot}} \right)^{6/5}, \quad (35)$$

$$J_t = 5.48 \times 10^{45} \text{ g cm}^2 \text{ s}^{-1} \alpha_{-1}^{-6/5} (x_{max}^{13/10} - 1) \times \left( \frac{\dot{M}}{10^{-3} M_{\odot} \text{ s}^{-1}} \right) \left( \frac{M_{BH}}{3 M_{\odot}} \right)^{11/5}. \quad (36)$$

For a given value of  $m_d$ ,  $J_t$ ,  $\alpha$ ,  $M_{BH}$ , from Eqs. (35) and (36), we can determine  $\dot{M}$  and  $x_{max}$  in general. Let us define a new variable  $\beta$  by  $J_t = m_d \beta \sqrt{GM_{BH} r_{ISCO}}$ , that is, the mean value of the angular momentum is  $\beta (> 1)$  times the minimum value of the specific angular momentum at the ISCO. Then,  $x_{max}$  is determined by

$$\frac{x_{max}^{13/10} - 1}{x_{max}^{4/5} - 1} = 1.625\beta. \quad (37)$$

It is easily shown that the l.h.s of Eq. (37) is a monotonically increasing function for  $x_{max} > 1$  and has a minimum value 1.625 at  $x_{max} = 1$  so that, for an arbitrary value of  $\beta > 1$ , there is a unique solution  $x_{max} > 1$ . In the accretion process, the total angular momentum of the system should be conserved in our case, since the Kerr metric has a rotational Killing vector, i.e., a stationary axisymmetric system. Some of the angular momentum is absorbed by the BH from the ISCO so that  $\beta$  increases as a function of time. Note that the spin up of the BH due to the accretion is negligible in our case. If we denote the mass and the angular momentum of the accreted blob into the BH as  $\Delta m_d (< 0)$  and  $\Delta J = \Delta m_d \sqrt{GM_{BH} r_{ISCO}}$ , we have

$$\Delta\beta = (1 - \beta) \frac{\Delta m_d}{m_d} > 0. \quad (38)$$

The solution of Eq. (38) is given by

$$\beta = 1 + (\beta_0 - 1) \frac{m_d^0}{m_d}, \quad (39)$$

where  $\beta_0$  and  $m_d^0$  are the initial values of  $\beta$  and  $m_d$ , respectively. Therefore,  $\beta \gg 1$  in the later phase of the accretion so that  $x_{max} \gg 1$  and the  $x_{max} \approx (1.6\beta)^2 \approx [1.6(\beta_0 - 1) \times m_d^0/m_d]^2$  will be a good approximation. Inserting this expression to Eq. (35), we have

$$\frac{\dot{m}_d}{m_d^{13/5}} = -3.47 \text{ s}^{-1} [m_d^0(\beta_0 - 1)]^{-8/5} \alpha_{-1}^{6/5} \left( \frac{M_{BH}}{3 M_{\odot}} \right)^{-6/5}. \quad (40)$$

Integration of Eq. (40) yields

$$m_d = \frac{m_d^0}{(t/A + 1)^{5/8}}, \quad (41)$$

$$A = 0.18 \text{ s} (\beta_0 - 1)^{8/5} \alpha_{-1}^{-6/5} \left( \frac{M_{BH}}{3 M_{\odot}} \right)^{6/5}, \quad (42)$$

$$\dot{m}_d = -\frac{5m_d^0}{8A(t/A + 1)^{13/8}}. \quad (43)$$

The method we adopted here to solve the evolution of the accretion disk is similar to the quasi static evolution of the star where the nuclear time scale is much longer than the free fall time so that at each time the star can be regarded in a gravitational equilibrium (see, e.g., Kippenhahn & Weigert 1994). In our case, from Eq. (32), the accretion velocity is much smaller than the Kepler velocity which determines the dynamical time scale so that we can regard the disk stationary at each time. The decrease of the total mass and the angular momentum can be regarded as the decrease of the total nuclear energy and the change of the composition in the stellar evolution case, which are very slowly changing in a dynamical time scale.

Let us assume that  $m_d^0 = 0.1 M_{\odot}$ ,  $\beta_0 = 2$ ,  $M_{BH} = 3 M_{\odot}$ , and  $q = 0.5$  as suggested by numerical relativity calculations (Shibata & Taniguchi 2006; Kiuchi et al. 2009; Rezzolla et al. 2010; Hotokezaka et al. 2011, 2013). Solid lines in Fig. 1 show the accretion rates as a function of  $\alpha$  for the representative time such as 1 s, 3 s, 10 s, 30 s, 100 s and 300 s. We are interested in the late time behavior ( $t > 30$  s) where the accretion rate decreases as a function of  $\alpha$  for a fixed time. This is because  $A$  in Eq. (42) is smaller for larger  $\alpha$  so that the accretion rate is smaller. Physically the accreting velocity is larger for larger viscosity as is clear from Eq. (31), where the consumption of the disk mass is faster. The dashed lines are neutrino cooling ignition accretion rate obtained by Chen & Beloborodov (2007) for  $q = 0$  and  $q = 0.95$  (Eq. 42 of their paper). Neutrino cooling is effective only above these dashed lines. In Fig. 2, we show BZ luminosity as a function of  $\alpha$  for typical time such as 1 s, 3 s, 10 s, 30 s, 100 s and 300 s for  $m_d^0 = 0.1 M_{\odot}$ ,  $\beta_0 = 2$ ,  $M_{BH} = 3 M_{\odot}$ , and  $q = 0.5$ . The magnetic field at the horizon is assumed to be determined by

$$\frac{B^2}{8\pi} = p_{ISCO}, \quad (44)$$

where  $p_{ISCO}$  is the pressure of the disk at the ISCO in Eq. (29). The BZ luminosity is then given by Eq. (10). We clearly see that the BZ luminosity is higher for smaller  $\alpha$  for the same time. This comes from both the strong  $\alpha$  dependence of the  $p_{ISCO}$  in Eq. (29) and the accretion rate in Fig. 1. Physically, if the viscosity is low, the accretion rate decreases slowly and the pressure is high due to the accumulation of the matter, which yield strong magnetic field in our scenario. All these effects result in a larger BZ luminosity for a smaller  $\alpha$ .

One might suspect that our approximation ( $x_{max} \gg 1$ ) to the solution of Eq. (37) for given  $\beta$  affects the result. To check this, we show in Fig. 3 the time evolution of the luminosity for  $m_d^0 = 0.1 M_{\odot}$ ,  $\beta_0 = 2$ ,  $M_{BH} = 3 M_{\odot}$ ,  $q = 0.5$ , and  $\alpha = 0.01$ . The red and blue solid



lines show the numerical exact solution and the analytic approximation, respectively. The dashed horizontal lines show the neutrino cooling ignition accretion rates for  $q = 0$  (upper) and  $q = 0.95$  (lower), respectively. We see that the analytic approximation only overestimates the luminosity slightly. We can justify the use of the analytic approximate solution to Eq. (37).

It is suggested that the typical  $\alpha \sim 0.01$ -0.02 from various numerical simulations (Davis et al. 2010; Guan & Gammie 2011; Blaes et al. 2011; Parkin & Bicknell 2013; Jiang et al. 2013). To have possible isotropic EE, the typical luminosity of  $\sim 10^{49}$  erg s $^{-1}$  is needed at  $t \sim 100$  s. If  $\alpha \sim 0.01$  as suggested by various numerical simulations, the luminosity at  $t = 100$  s is above  $\sim 10^{50}$  erg s $^{-1}$  so that the enough luminosity seems to be obtained by BZ mechanism. However, from Fig. 1, the accretion rate is above the ignition rate for neutrino cooling only up to  $t \sim 30$  s. In this case the duration of EE is at most 30 s. To increase the duration of EE, we need smaller  $\alpha$  than 0.01. When can the value of  $\alpha$  become smaller? If the origin of viscosity is magnetic turbulence from the magneto rotational instability, there is a big difference from the usual situations, that is, the matter is neutron rich ( $Y_e \sim 0.1$ ). Since neutron does not directly couple to the magnetic field, and  $Y_e \sim 0.1$ , only 10% of the mass feels the viscosity first. Note that, for  $T \sim 10^{10}$  K,  $B \sim 10^{15}$  G,  $\rho \sim 10^{10}$  g cm $^{-3}$ , which are typical values at the ISCO, the gyration radius of the proton  $\sim 10^{-10}$  cm is comparable to the mean free path of p-n collision with the cross section of  $\sim 1$  barn. Then, the effective  $\alpha_{eff}$  might be reduced, in principle, 10% compared to the usual case of proton (= hydrogen) dominated gas, i.e.,  $\alpha \sim 0.01$  in the conventional definition could give  $\alpha_{eff} \sim 0.001$ . Then, from Fig. 1, the duration can be even longer than  $\sim 100$  s and the BZ luminosity can supply an enough energy for the isotropic EE. These arguments suggest that the rotational energy of the Kerr BHs formed in compact binary mergers might supply the energy sources of the EEs with the required duration even if the emissions are isotropic.

In Newtonian gravity, there exists the numerical simulation of the accretion disk for the present problem, i.e., the time evolution of the accretion disk of mass  $0.1 M_\odot$  after the merger of NS-NS binary (Metzger et al. 2009). Our treatment is also using Newtonian gravity so that we can compare our analytic results with their numerical simulations to confirm the quantitative agreement. In their simulations the mass of the central BH is  $3 M_\odot$  and they solved the time evolution of the z-direction integrated quantity such as the surface density  $\Sigma$  with neutrino and advection cooling. The initial surface density is given as

$$\Sigma \propto (r/r_{d,0})^5 \exp(-7r/r_{d,0}), \quad (45)$$

with  $r_{d,0} = 3 \times 10^6$  cm  $\sim 6GM_{BH}/c^2$ . Since  $\Sigma r^2$  peaks at  $r_{d,0}$ , the initial specific angular momentum is  $\sim \sqrt{GM_{BH} \times 6GM_{BH}/c^2}$ . In our crude model, we assumed the disk boundary is at  $r_{ISCO} = 6GM_{BH}/c^2$  while in their simulation inner edge (= disk boundary) is  $10^6$  cm  $\sim 2GM_{BH}/c^2$  so that we define the coordinate  $x$  by  $r = x \times 2GM_{BH}/c^2$  in this paragraph. In the Newtonian simulation, there is no ISCO so that the

minimum specific angular momentum of their simulation is  $\sim \sqrt{GM_{BH} \times 2GM_{BH}/c^2}$  which is different from our model of  $\sqrt{GM_{BH} \times 6GM_{BH}/c^2}$ . As for  $\alpha$  they adopt 0.3 so that we need to rewrite Eqs. (35) and (36) as

$$m_d = 1.53 \times 10^{-5} M_\odot (x_{max}^{4/5} - 1) \times \left( \frac{\dot{M}}{10^{-3} M_\odot s^{-1}} \right) \left( \frac{M_{BH}}{3 M_\odot} \right)^{6/5}, \quad (46)$$

$$J_t = 3.52 \times 10^{44} \text{ g cm}^2 \text{ s}^{-1} (x_{max}^{13/10} - 1) \times \left( \frac{\dot{M}}{10^{-3} M_\odot s^{-1}} \right) \left( \frac{M_{BH}}{3 M_\odot} \right)^{11/5}. \quad (47)$$

Defining  $\beta$  by  $J_t = m_d \beta \sqrt{GM_{BH} \times 2GM_{BH}/c^2}$ , we have the same equation as Eq. (37). The argument to derive equations corresponding to Eqs. (38) and (39) is also the same by changing  $\Delta J = \Delta m_d \sqrt{GM_{BH} \times 2GM_{BH}/c^2}$  and  $\beta_0 \sim \sqrt{3}$ , which gives

$$\frac{\dot{m}_d}{m_d^{13/5}} = -51.0 \text{ s}^{-1} (m_d^0)^{-8/5} \left( \frac{M_{BH}}{3 M_\odot} \right)^{-6/5}. \quad (48)$$

Integration of Eq. (48) yields

$$m_d = 0.1 M_\odot \left( \frac{t}{1.22 \times 10^{-2} \text{ s}} + 1 \right)^{-5/8}, \quad (49)$$

$$\dot{m}_d = -5.12 M_\odot \text{ s}^{-1} \left( \frac{t}{1.22 \times 10^{-2} \text{ s}} + 1 \right)^{-13/8}. \quad (50)$$

Now let us compare Eq. (50) with those of the numerical simulations by Metzger et al. (2009). Their Fig. 3 shows the accretion rate at  $r = 10^6$  cm for  $t = 0.01$  s, 0.1 s and 1 s are  $1 M_\odot \text{ s}^{-1}$ ,  $0.1 M_\odot \text{ s}^{-1}$  and  $4.5 \times 10^{-3} M_\odot \text{ s}^{-1}$ , respectively. While Eq. (50) yields  $1.93 M_\odot \text{ s}^{-1}$ ,  $0.139 M_\odot \text{ s}^{-1}$  and  $3.9 \times 10^{-3} M_\odot \text{ s}^{-1}$ . We can say that our analytic model agrees rather well with the numerical simulations at ISCO especially for later times, which is indispensable for the use of our analytic model to study EE.

### 3. EXTENDED X-RAY EMISSION AS AN ELECTROMAGNETIC COUNTERPART OF COMPACT BINARY MERGER

In the previous section, we show that the rotational energy of the Kerr BH up to  $E_{BZ} \sim 10^{53}$  erg can be extracted as the Poynting outflow via the BZ process with a time scale of  $\delta t_{BZ} \sim 100$  s if the accretion of the debris  $\sim 0.1 M_\odot$  occurs with  $\alpha \sim 0.01$ . Hereafter, we argue resultant emissions from such outflows and their detectability.

In the course of compact binary mergers, a fraction of baryons of mass  $M \sim 10^{-(2-4)} M_\odot$  can be ejected with an expansion velocity of  $v_{exp} \sim 0.1c$  (Hotokezaka et al. 2013). A certain duration after the merger, say  $\delta t \sim 0.1$  s, the hypermassive NS collapse into a BH due to the loss of the rotational support by emitting gravitational waves (GWs) and/or Poynting fluxes. The Poynting outflow or jet by the BZ process, which is relativistic, clashes with the pre-ejecta, and a significant fraction of

the Poynting energy can dissipate into heat, which predominantly occurs at

$$r_o \lesssim c\delta t_{BZ} \sim 3.0 \times 10^{12} \text{ cm } \delta t_{BZ,2}, \quad (51)$$

where  $\delta t_{BZ}$  corresponds to the time  $t$  in the previous section. After the dissipation, the heated pre-ejecta can be regarded as a fireball. The temperature can be estimated as  $T'_o \approx (3\xi E_{BZ}/a_{rad}\Delta\Omega r_o^2\delta t_{BZ}c)^{1/4}$ , or

$$k_B T'_o \sim 2.9 \text{ keV } \xi_{-1}^{1/4} E_{BZ,53}^{1/4} \delta t_{BZ,2}^{-1/4} \Delta\Omega^{-1/4} r_{o,12}^{-1/2}, \quad (52)$$

where  $\Delta\Omega$  is the beaming factor of the fireball which is  $4\pi$  for the isotropic case and  $\xi$  is the efficiency factor. We note that the optical depth at around this radius is large,  $\tau_T \approx Y_e \kappa_T \rho r \sim 4.2 \times 10^7 (Y_e/0.2) M_{-2} r_{12}^{-1} \delta t_{-1}$ . Here,  $\kappa_T \sim 0.2 \text{ g}^{-1} \text{ cm}^2$  is the opacity of the Thomson scattering,  $\rho \approx M/4\pi r^2 c \delta t \sim 5.3 \times 10^{-4} M_{-2} r_{12}^{-2} \delta t_{-1} \text{ g cm}^{-3}$  is the mean density of the ejecta, and  $M_{-2} = M/10^{-2} M_\odot$  is the isotropic mass ejection. Though the mass ejection, in general, is unisotropic (e.g. Hotokezaka et al. 2013), we can take into account this effect by changing  $\Delta\Omega$  and  $M$  appropriately. The fireball is accelerated due to the large internal energy, and the Lorentz factor saturates at  $\Gamma \sim 4\pi\xi E_{BZ}/\Delta\Omega M c^2$ , or

$$\Gamma \sim 7.0 \xi_{-1} E_{BZ,53} M_{-2}^{-1} \Delta\Omega^{-1}, \quad (53)$$

which occurs at

$$r_s \approx r_o \Gamma \sim 7.0 \times 10^{12} \text{ cm } \xi_{-1} E_{BZ,53} M_{-2}^{-1} \Delta\Omega^{-1} r_{o,12}. \quad (54)$$

Hereafter, we simply assume  $\Gamma \propto r$  in the acceleration phase.<sup>7</sup> For  $r > r_s$ , the fireball moves as a shell with the shell width  $\sim r_s$  so that the temperature decreases as  $T' \propto (r/r_s)^{-2/3}$ , while in the lateral direction  $y$ , it expands as  $y \sim r/\Gamma$  (e.g., Mészáros & Rees 2000). Then, the fireball begins to expand almost spherically irrespective of the initial beaming angle beyond the radius given by

$$r_{exp} \approx r_s \Gamma \sim 4.9 \times 10^{13} \text{ cm } \xi_{-1}^2 E_{BZ,53}^2 M_{-2}^{-2} \Delta\Omega^{-2} r_{o,12}. \quad (55)$$

The temperature decreases as  $T' \propto (r/r_{exp})^{-1}$  for  $r > r_{exp}$ .

The photospheric emission from the fireball can be expected around the photospheric radius,

$$r_{ph} \approx \left( \frac{Y_e \kappa_T M}{4\pi} \right)^{1/2} \sim 2.5 \times 10^{14} \text{ cm } (Y_e/0.2)^{1/2} M_{-2}^{1/2}. \quad (56)$$

The temperature of the fireball in the comoving frame evolves as  $T' \propto (r/r_o)^{-1}$  for  $r_o < r < r_s$ ,  $T' \propto (r/r_s)^{-2/3}$  for  $r_s < r < r_{exp}$ , and  $T' \propto (r/r_{exp})^{-1}$  for  $r_{exp} < r$ . From Eqs. (55) and (56),  $r_{ph} > r_{exp}$  is satisfied if  $M$  is larger than the critical mass given by

$$M_{-2} > 0.76 (Y_e/0.2)^{-1/5} \xi_{-1}^{4/5} E_{BZ,53}^{4/5} \Delta\Omega^{-4/5} r_{o,12}^{2/5}. \quad (57)$$

In the case of *dirty* fireballs with  $M_{-2} \sim 1$ ,  $r_{ph} > r_{exp}$  is expected. The temperature at the photospheric radius

<sup>7</sup> If only a tiny fraction of Poynting energies is dissipated at  $r \sim r_o$ , the fireball is still magnetically dominated, and the evolution of the Lorentz factor is different from the above scaling, in general;  $\Gamma \propto r^\mu$  with  $1/3 \lesssim \mu \lesssim 1$ .

becomes  $T'_{ph} \approx T'_o (r_s/r_o)^{-1} (r_{exp}/r_s)^{-2/3} (r_{ph}/r_{exp})^{-1}$ , which is expressed as

$$k_B T'_{ph} \sim 22 \text{ eV } (Y_e/0.2)^{-1/2} \times \xi_{-1}^{7/12} E_{BZ,53}^{7/12} M_{-2}^{-5/6} \delta t_{BZ,2}^{-1/4} \Delta\Omega^{-7/12} r_{o,12}^{1/2}, \quad (58)$$

and the peak photon energy of the resultant photospheric emission can be estimated as  $\varepsilon_{peak} \approx 2.83 k_B T'_{ph} \Gamma / (1+z)$ , which is given by

$$\varepsilon_{peak} \sim 0.40 \text{ keV } (1+z)^{-1} (Y_e/0.2)^{-1/2} \times \xi_{-1}^{19/12} E_{BZ,53}^{19/12} M_{-2}^{-11/6} \delta t_{BZ,2}^{-1/4} \Delta\Omega^{-19/12} r_{o,12}^{1/2}. \quad (59)$$

The peak intensity in the comoving frame can be approximated as  $I'_{peak} \approx 2(\nu'_{peak}/c)^2 \times 2.83 k_B T'_{ph} \times \exp(-2.83)$ , where  $\nu'_{peak} \approx 2.83 k_B T'_{ph}/h$  with the Planck constant  $h = 6.62 \times 10^{-27} \text{ erg s}$ .<sup>8</sup> In the observer frame, using the fact that  $I_\nu/\nu^3$  is Lorentz invariant (e.g., Rybicki & Lightman 1979), the corresponding energy flux is given by  $F_{peak} \approx (\pi/\Gamma^2) \times (r_{ph}/d_L)^2 \times \Gamma^3 \times I'_{peak} \times (1+z)$  with  $d_L$  and  $1/\Gamma^2$  being the luminosity distance and the relativistic beaming effect, respectively, as

$$F_{peak} \approx 0.37 \times \frac{(1+z)^4}{\Gamma^2} \left( \frac{r_{ph}}{d_L} \right)^2 \frac{\varepsilon_{peak}^3}{h^2 c^2} \sim 1.1 \times 10^{-23} \text{ erg cm}^{-2} \text{ s}^{-1} \text{ Hz}^{-1} (1+z) \times \left( \frac{d_L}{200 \text{ Mpc}} \right)^{-2} (Y_e/0.1)^{-1/2} \times \xi_{-1}^{11/4} E_{BZ,53}^{11/4} M_{-2}^{-5/2} \delta t_{BZ,2}^{-3/4} \Delta\Omega^{-11/4} r_{o,12}^{3/2}, \quad (60)$$

$$\nu_{peak} F_{peak} \sim 1.2 \times 10^{-6} \text{ erg cm}^{-2} \text{ s}^{-1} \times \left( \frac{d_L}{200 \text{ Mpc}} \right)^{-2} (Y_e/0.1)^{-1} \times \xi_{-1}^{13/3} E_{BZ,53}^{13/3} M_{-2}^{-13/3} \delta t_{BZ,2}^{-1} \Delta\Omega^{-13/3} r_{o,12}^2. \quad (61)$$

The observed duration of the photospheric emission is given by

$$t_{dur} \approx (1+z) \times \max[r_{ph}/c\Gamma^2, \delta t_{BZ}]. \quad (62)$$

In the case of dirty fireballs, the first term in the r.h.s of the above equation always larger than the second one, thus,

$$t_{dur} \sim 170 \text{ s } (1+z) (Y_e/0.2)^{1/2} \xi_{-1}^{-2} E_{BZ,53}^{-2} M_{-2}^{5/2} \Delta\Omega^2. \quad (63)$$

We remark that the EE duration of  $t_{dur} > 100 \text{ s}$  do not necessarily require the duration of the BZ jet of  $\delta t_{BZ} > 100 \text{ s}$  if the fireball is dirty and the duration is determined by Eq. (63). For a fiducial parameter set ( $\xi = 0.1, E_{BZ,53} = 1, M_{-2} = 1, \delta t_{BZ,2} = 1, \Delta\Omega = 1$ ), the emission is characterized by  $\varepsilon_{peak} \sim 0.42 \text{ keV}$ ,  $\nu_{peak} F_{peak} \sim 1.2 \times 10^{-6} \text{ erg cm}^{-2} \text{ s}^{-1}$ , and  $t_{dur} \sim 180 \text{ s}$  from  $d_L = 200 \text{ Mpc}$ , and  $\varepsilon_{peak} \sim 0.29 \text{ keV}$ ,  $\nu_{peak} F_{peak} \sim 6.0 \times 10^{-9} \text{ erg cm}^{-2} \text{ s}^{-1}$ , and  $t_{dur} \sim 260 \text{ s}$  from  $z = 0.5$ .

<sup>8</sup> Note that here  $h$  is not the half thickness of the disk but the Planck constant. Also we use  $\beta$  as the spectral index in this section.

In general, the spectral shape is determined by additional dissipation processes, e.g., internal shocks or magnetic reconnections, occurring in  $r_o < r < r_{ph}$ , which may slightly boost the peak energy and most likely produce a quasi-thermal spectrum,

$$F \approx F_{peak} \times \begin{cases} (\varepsilon/\varepsilon_{peak})^2 & \text{for } \varepsilon < \varepsilon_{peak}, \\ (\varepsilon/\varepsilon_{peak})^\beta, & \text{for } \varepsilon_{peak} < \varepsilon < \varepsilon_{cut}. \end{cases} \quad (64)$$

For example, Pe'er et al. (2006) numerically calculated the photospheric emission from fireballs (in their cases, hot-plasma cocoon) including some dissipation processes at  $r \lesssim r_{ph}$ , and show that typically  $\beta \sim -1$  and  $\varepsilon_{cut} \sim 30 \times \varepsilon_{peak}$ . Then, for our fiducial parameters,  $\varepsilon_{cut} \sim 13$  keV from  $d_L = 200$  Mpc so that the spectrum may range from  $\sim 0.4$  keV to  $\sim 13$  keV. We plot the possible  $\nu F_\nu$  spectra in Fig. 4. Though  $\varepsilon_{peak}$  has parameter dependancies as Eq. (59), it is most likely that  $\varepsilon_{cut}$  is below 15 keV for  $M_{-2} \sim 1$  and  $\Delta\Omega \sim 1$ . In this case, the emission energy is outside of the coverage of BATSE and *Swift* BAT so that such EEs have not been detected so far. On the other hand, the soft EEs can be detected by soft X-ray survey facilities like Wide-Field MAXI (Kawai 2013), which has a  $0.1^\circ$  angular resolution.

Let us estimate the possible detection rate of the soft EEs discussed above, in particular, simultaneously with the GWs from compact binary mergers;

$$0.2 \times 0.8 \times 0.9 \times f_{softEE} \left( \frac{\Delta\Omega_{softEE}}{4\pi} \right) \mathcal{R}_{GW} \\ \sim 5.7 \text{ yr}^{-1} f_{softEE} \left( \frac{\Delta\Omega_{softEE}}{4\pi} \right) \left( \frac{\mathcal{R}_{GW}}{40 \text{ yr}^{-1}} \right), \quad (65)$$

where  $f_{softEE}$  is the fraction of the soft EEs in all SGRBs, and  $\mathcal{R}_{GW}$  represents the NS-NS merger rate within the detection horizon of advanced LIGO, advanced VIRGO, and KAGRA,  $d_L \sim 200$  Mpc, which corresponds to a redshift of  $z \sim 0.046$  and a comoving volume of  $V_{GW} \sim 0.03$  Gpc<sup>3</sup>. We assume the standard  $\Lambda$ -CDM cosmology. Note here that  $f_{softEE} \sim 1$  can be expected given that the fraction of EE burst is significantly larger in softer energy bands;  $\sim 25\%$  in the *Swift* BAT samples ( $> 15$  keV) and  $\sim 7\%$  in the BATSE samples ( $> 20$  keV). We take into account the sky coverage of Wide-Field MAXI  $\sim 20\%$  and the anticipated duty cycle,  $\sim 80\%$  for Wide-Field MAXI and  $\sim 90\%$  for the 2nd generation GW network. In the case of dirty fireballs, the beaming factor can be relatively large, e.g.,  $\Delta\Omega_{softEE} \sim 1$ , and the above estimate gives  $\sim 0.5 \text{ yr}^{-1}$  for  $\mathcal{R}_{GW} \sim 40 \text{ yr}^{-1}$  and  $f_{softEE} \sim 1$ . With a planned detection threshold flux of Wide-Field MAXI  $\sim 1.0 \times 10^{-9} \text{ erg s}^{-1} \text{ cm}^{-2}$ , such soft EEs can be detectable from  $z \sim 0.5$ , which corresponds to a luminosity distance of  $d_L = 2.8$  Gpc and a comoving volume of  $V_{softEE,MAXI} = 28$  Gpc<sup>3</sup>. The anticipated total detection rate can be estimated as

$$\sim 430 \text{ yr}^{-1} f_{softEE} \Delta\Omega_{softEE} (\mathcal{R}_{GW}/40 \text{ yr}^{-1}). \quad (66)$$

Next let us consider the observed EEs in our scenario. As we argued above, the dissipative photospheric emissions from dirty fireballs are too soft and too dim for *Swift* BAT as far as  $M_{-2} \sim 1$  and  $\Delta\Omega \sim 1$ . Importantly, the typical beaming angle of the observed EEs

can be estimated much smaller as follows. The EEs are being detected predominantly by *Swift* BAT with the image trigger. Here we set the trigger threshold as 2 photon cm<sup>-2</sup> in 64 s (Toma et al. 2011). In this case, the trigger threshold by BAT for the burst with  $\beta = -1$  can be calculated as  $F_{det,BAT} = 1.9 \times 10^{-9} \text{ erg s}^{-1} \text{ cm}^{-2}$ . For an EE with a mean luminosity of  $L_{iso,15-150 \text{ keV}} \sim 10^{49} \text{ erg s}^{-1}$  (like SGRB 061006), the detection horizon also becomes  $d_L = 6.6$  Gpc, corresponding to  $z = 1$  and  $V_{EE,BAT} = 150$  Gpc<sup>3</sup>. For an effective total observation time of BAT as  $T_{obs,BAT} \sim 0.8 \times 6 \text{ yr}$ , and the sky coverage of the BAT as 15%, the total number of detectable EE becomes  $\sim 1.4 \times 10^5$  ( $\mathcal{R}_{GW}/40 \text{ yr}^{-1}$ ). Given that 14 EEs have been identified in this interval (Gompertz et al. 2013), the fraction of EE bursts  $f_{EE}$  and the beaming factor  $\Delta\Omega_{EE}/4\pi$  can be constrained as  $f_{EE}(\Delta\Omega_{EE}/4\pi) \sim 9.7 \times 10^{-5} (\mathcal{R}_{GW}/40 \text{ yr}^{-1})^{-1}$ , or

$$\Delta\Omega_{EE} \sim 4.9 \times 10^{-3} \left( \frac{f_{EE}}{0.25} \right)^{-1} \left( \frac{\mathcal{R}_{GW}}{40 \text{ yr}^{-1}} \right)^{-1}, \quad (67)$$

which is comparably small as the inferred beaming factor of the prompt spikes,  $\Delta\Omega_{PS}/4\pi \sim 10^{-3}$  (Fong et al. 2012). We should mention that candidates of "orphan" EEs without prompt spikes, i.e., long GRBs with  $T_{90} \gtrsim 100$  whose redshifts and host galaxies are not identified, have been detected by *Swift* BAT. The detection rate of those candidates is roughly comparable to that of SGRBs with EEs<sup>9</sup>. Given this fact, the constraint on the beaming factor (Eq. 67) is a lower limit and can be larger by a factor. Nevertheless, the possible simultaneous detection rate of such EEs and GWs from NS-NS mergers would be quite small,  $\approx 0.15 \times 0.8 \times 0.9 \times \mathcal{R}_{GW} f_{EE}(\Delta\Omega_{EE}/4\pi) \lesssim 10^{-3} \text{ yr}^{-1}$ . Note that the estimated value is independent of relatively uncertain binary NS merger rate.

In the context of our picture, a smaller  $\Delta\Omega$  corresponds to a relatively narrow fireball. We note that the mass ejection associated for the BH-NS merger is orders-of-magnitude smaller in the polar direction than the angle averaged one, which have been confirmed by numerical simulations (Kyutoku et al. 2013) where the BH spin is set to be parallel to the orbital angular momentum. In general, it is expected that they are misaligned due to the kick velocity in the formation process of NSs. Although more numerical simulations using general initial conditions are needed to know what happens in BH-NS mergers, the simulations by Kyutoku et al. (2013) suggests that the matter along BZ jet axis is small compared with NS-NS binary. As a result, one can expect that a smaller fraction of energy is dissipated in a smaller region of the pre-ejecta compared with the previous NS-NS cases where the outflows via the BZ process clash with denser pre-ejecta. Hereafter, we take  $\xi \sim 10^{-4}$ ,  $M \sim 10^{-4} M_\odot$ ,  $\Delta\Omega \sim 10^{-2}$  as a fiducial value.

Such fireballs are *clean* in that  $r_{ph} < r_s$ , i.e.,

$$M_{-4} < 2.3 (Y_e/0.2)^{-1/3} \xi_{-4}^{2/3} E_{BZ,53}^{2/3} \Delta\Omega_{-2}^{-2/3} \delta r_{o,12}^{2/3}. \quad (68)$$

The Lorentz factor of such clean fireballs and the comoving temperature at the photospheric radius are  $T'_{ph} \approx T'_o(r_{ph}/r_o)^{-1}$  and  $\Gamma \approx r_{ph}/r_o$ , respectively, and the peak energy of the photospheric emission  $\varepsilon_{peak} \approx 2.83 k_B T'_{ph} \times$

<sup>9</sup> <http://swift.gsfc.nasa.gov/archive/grbtable/>



$\Gamma/(1+z)$  can be estimated as

$$\varepsilon_{peak} \sim 4.3 \text{ keV } (1+z)^{-1} \xi_{-1}^{1/4} E_{BZ,53}^{1/4} \delta t_{BZ,2}^{-1/4} \Delta\Omega^{-1/4} r_{o,12}^{-1/2}. \quad (69)$$

From Eq. (60), the corresponding peak flux is

$$\begin{aligned} \nu_{peak} F_{peak} &\sim 1.0 \times 10^{-5} \text{ erg cm}^{-2} \text{ s}^{-1} \\ &\times \left( \frac{d_L}{200 \text{ Mpc}} \right)^{-2} \\ &\times \xi_{-4} E_{BZ,53} \delta t_{BZ,2}^{-1} \Delta\Omega_{-2}^{-1}. \end{aligned} \quad (70)$$

In the case of clean fireballs, the emission duration is  $t_{dur} \approx (1+z) \times \delta t_{BZ}$ .

For a fiducial parameter set ( $\xi = 10^{-4}$ ,  $E_{BZ,53} = 1$ ,  $M_{-4} = 1$ ,  $\delta t_{BZ,2} = 0.7$ ,  $\Delta\Omega_{-2} = 1$ ), the emission is characterized by  $\varepsilon_{peak} \sim 3.5 \text{ keV}$ ,  $\nu_{peak} F_{peak} \sim 1.2 \times 10^{-7} \text{ erg cm}^{-2} \text{ s}^{-1}$ , and  $t_{dur} \sim 100 \text{ s}$  from  $z = 0.4337$  (see Fig. 4 where we also plot an observed flux spectrum of EE associated with SGRB 061006 at  $z = 0.4337$ ). The observed EEs can be consistently interpreted as the high energy tail of the photospheric emission from such a clean fireball. To test this scenario, the simultaneous detections in the soft X-ray band ( $< 10 \text{ keV}$ ) is crucial.

#### 4. DISCUSSIONS

As for the EEs from fireballs, we need to model e.g., the subphotospheric dissipation processes, in detail to predict the spectra more precisely. Nevertheless, a key message here is that the typical energy of EEs are likely to be in soft X-ray bands. In our scenario, this is essentially due to the relatively large launching radii of the fireball,  $r_o \sim 10^{12} \text{ cm}$  (Eq. 51) compared with that of the conventional GRB fireball,  $r_o \sim 10^7 \text{ cm}$ , which results in a lower initial temperature (Eq. 52). The importance of soft X-ray bands have been implied from the observed soft photon index of EE and the increase of the fraction of SGRB with EE in softer bands. We strongly encourage soft X-ray survey facilities like Wide-Field MAXI, which can provide a useful electromagnetic counterpart of the GWs from compact binary mergers with an angular resolution of  $\sim 0.1^\circ$ . Such EE counterparts are also important in terms of time domain astronomy since they would be observed only an  $\sim 1 \text{ s}$  after the mergers. If a larger detection rate as Eq. (66) is realized, a statistical technique using a stacking approach might also be possible for the detection of the GWs, with the aid of the soft EE counterparts. One might think that soft EEs should have been already detected by MAXI<sup>10</sup>, though the rapid sky sweeping ( $\sim 4\pi/90 \text{ min}$ ) makes it difficult to identify the  $\sim 100 \text{ s}$  emissions.

In the present paper, we treated the accretion disk in a Newtonian gravity for a constant accretion rate at first, then required that the finite total disk mass and the total angular momentum. Then, we solved the evolution of the size of the disk and the accretion rate. This treatment should be regarded as a crude approximation, and we should compare our results with the numerical simulations. Unfortunately we could not find the numerical simulations of the evolution of finite size accretion disk either in Kerr or Schwarzschild metric in the literature.

<sup>10</sup> <http://maxi.riken.jp/top/>

One of the basic problem here is the relativistic treatment of the  $\alpha$  viscosity. The simple generalization of the Navier Stokes equation such as done in the text book, for example, *Fluid mechanics* (chapter 127) by Landau & Lifshitz violates the causality (Israel 1976), i.e., the information propagates with the speed faster than the light velocity. The reason is simple and clear. Let us consider the non-relativistic one dimensional diffusion equation for some quantity  $Q(t, x)$ ,

$$\frac{\partial Q}{\partial t} = D \frac{\partial^2 Q}{\partial x^2}, \quad (71)$$

where  $D$  is the diffusion constant. If we put the delta function source such as

$$\frac{\partial^2 Q}{\partial x^2} - D^{-1} \frac{\partial Q}{\partial t} = -C \delta(x) \delta(t), \quad (72)$$

the solution for  $t > 0$  is expressed as

$$Q = C \sqrt{\frac{1}{4\pi Dt}} \exp\left(-\frac{x^2}{4Dt}\right). \quad (73)$$

The above solution clearly shows that the initial disturbance at  $t = 0$  and  $x = 0$ , propagates to any  $x$  even for any very small value of  $t > 0$ , which means the causality is violated, i.e., the information propagates with the infinite speed. The simple rule to make the non-relativistic equation to general relativistic one such as changing the derivative to the covariant derivative and the use of the projection of the tensor using  $p^{\mu\nu} \equiv g^{\mu\nu} + u^\mu u^\nu$  do not help to guarantee the causality. We need to add several new terms with undetermined parameters to the basic equations such as done by Israel & Stewart (1979). If we can start from the general relativistic Boltzmann equation, there is no problem as for the causality in principle. However, in practice, we should treat the distribution function that depends on three coordinates and three momenta, which is beyond the ability of the present computer power to simulate such a problem. One may think that the general relativistic resistive MHD simulations in 3D are enough to solve this problem since the causality is not violated in such a system. However, the Boltzmann equation should be solved anyway since the gyration radius of the proton is typically comparable to the mean free path of p-n collision at around the ISCO.

#### 5. ACKNOWLEDGEMENTS

The authors would like to thank Kunihiro Ioka, Tsvi Piran, Norita Kawanaka, Kenta Hotokezaka, Hiroki Nagakura, Koutaro Kyutoku, Peter Meszaros, Peter Veres, Shuichi Inutsuka, Makoto Takamoto, and Sanemichi Takahashi for useful comments. This work is supported in part by the Grant-in-Aid from the Ministry of Education, Culture, Sports, Science and Technology (MEXT) of Japan, No.23540305 (T.N.), No.24103006 (T.N.), No.23840023 (Y.S.) and JSPS fellowship (K.K.).

#### REFERENCES

- Blaes, O., Krolik, J. H., Hirose, S., & Shabaltas, N. 2011, ApJ, 733, 110
- Blandford, R. D., & Znajek, R. L. 1977, MNRAS, 179, 433
- Bostanci, Z. F., Kaneko, Y., Gogus, E. 2013, MNRAS, 428, 1623
- Bucciantini, N., Metzger, B. D., Thompson, T. A., & Quataert, E. 2012, MNRAS, 419, 1537



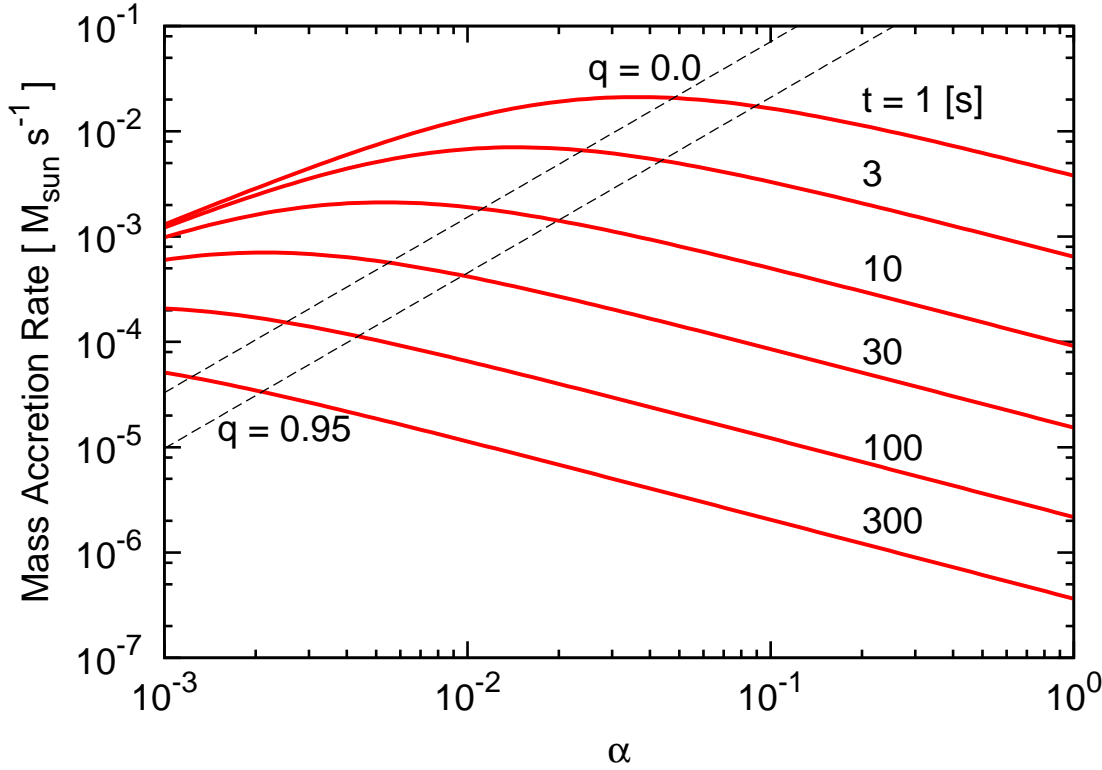


**Figure 1.** Accretion rate as a function of  $\alpha$  for typical time such as 1 s, 3 s, 10 s, 30 s, 100 s and 300 s for  $m_d^0 = 0.1 M_\odot$ ,  $\beta_0 = 2$ ,  $M_{BH} = 3 M_\odot$ . The dashed lines are neutrino cooling ignition accretion rate obtained by Chen & Beloborodov (2007) for  $q = 0$  and  $q = 0.95$  (Eq. 42 of their paper). Neutrino cooling is effective only above these dashed lines.

- Chen, W.-X., & Beloborodov, A. M. 2007, *ApJ*, 657, 383
- Davis, S. W., Stone, J. M., & Pessah, M. E. 2010, *ApJ*, 713, 52
- Eichler, D., Livio, M., Piran, T., & Schramm, D. N. 1989, *Nature*, 340, 126
- Fong, W., Berger, E., Margutti, R., et al. 2012, *ApJ*, 756, 189
- Fong, W., Berger, E., Chornock, R., et al. 2013, *ApJ*, 769, 56
- Fong, W., Berger, E., Chornock, R. et al. 2013, *ApJ*, 369, 56
- Gao, W.-H., & Fan, Y.-Z. 2006, *Chinese J. Astron. Astrophysics*, 6, 513
- Gompertz, B. P., O'Brien, P. T., Wynn, G. A., & Rowlinson, A. 2013, *MNRAS*, 431, 1745
- Goodman, J. 1986, *ApJ*, 308, L47
- Guan, X., & Gammie, C. F. 2011, *ApJ*, 728, 130
- Hotokezaka, K., Kyutoku, K., Okawa, H., Shibata, M., & Kiuchi, K. 2011, *Phys. Rev. D*, 83, 124008
- Hotokezaka, K., Kiuchi, K., Kyutoku, K., et al. 2013, *Phys. Rev. D*, 87, 024001
- Israel, W. 1976, *Annals of Physics*, 100, 310
- Israel, W., & Stewart, J. M. 1979, *Annals of Physics*, 118, 341
- Itoh, N., Adachi, T., Nakagawa, M., Kohyama, Y., & Munakata, H. 1989, *ApJ*, 339, 354
- Jiang, Y.-F., Stone, J. M., & Davis, S. W. 2013, *ApJ*, 767, 148
- Kawi, N. 2013, <http://spacephysics.uah.edu/gammacon/wp-content/program/programshibata7.htm>
- Kawanaka, N., Piran, T., & Krolik, J. H. 2013, *ApJ*, 766, 31
- Kippenhahn, R., & Weigert, A. 1994, *Stellar Structure and Evolution*, §9. Springer-Verlag Berlin Heidelberg New York. Also *Astronomy and Astrophysics Library*
- Kiuchi, K., Sekiguchi, Y., Shibata, M., & Taniguchi, K. 2009, *Phys. Rev. D*, 80, 064037
- Kouveliotou, C., Meegan, C. A., Fishman, G. J., et al. 1993, *ApJ*, 413, L101
- Kyutoku, K., Ioka, K., & Shibata, M. 2013, *Phys. Rev. D*, 88, 041503
- Metzger, B. D., Quataert, E., & Thompson, T. A. 2008, *MNRAS*, 385, 1455
- Metzger, B. D., Piro, A. L., & Quataert, E. 2009, *MNRAS*, 396, 304
- Mészáros, P., & Rees, M. J. 2000, *ApJ*, 530, 292
- Misner, C. W., Thorne, K. S., & Wheeler, J. A. 1973, *San Francisco: W.H. Freeman and Co.*, 1973,
- Narayan, R., Paczynski, B., & Piran, T. 1992, *ApJ*, 395, L83
- Paczynski, B. 1986, *ApJ*, 308, L43
- Parkin, E. R., & Bicknell, G. V. 2013, *MNRAS*, 435, 2281
- Pe'er, A., Mészáros, P., & Rees, M. J. 2006, *ApJ*, 652, 482
- Penna, R. F., Narayan, R., & Sądowski, A. 2013, *MNRAS*, 2531
- Perley, D. A., Metzger, B. D., Granot, J., et al. 2009, *ApJ*, 696, 1871
- Popham, R., Woosley, S. E., & Fryer, C. 1999, *ApJ*, 518, 356
- Rezzolla, L., Baiotti, L., Giacomazzo, B., Link, D., & Font, J. A. 2010, *Classical and Quantum Gravity*, 27, 114105
- Rybicki, G. B., & Lightman, A. P. 1979, *New York, Wiley-Interscience, "Radiation Processes in Astrophysics"* John Wiley & Sons §1.3 and 4.9
- Sakamoto, T., Barthelmy, S. D., Baumgartner, W. H., et al. 2011, *ApJS*, 195, 2
- Shakura, N. I., & Sunyaev, R. A. 1973, *A&A*, 24, 337
- Shibata, M., & Taniguchi, K. 2006, *Phys. Rev. D*, 73, 064027
- Toma, K., Sakamoto, T., & Mészáros, P. 2011, *ApJ*, 731, 127
- Tsutsui, R., Yonetoku, D., Nakamura, T., Takahashi, K., & Morioka, Y. 2013, *MNRAS*, 431, 1398
- Usov, V. V. 1992, *Nature*, 357, 472
- Villasenor, J. S., Lamb, D. Q., Ricker, G. R., et al. 2005, *Nature*, 437, 855
- Zhang, B., & Mészáros, P. 2001, *ApJ*, 552, L35
- Zhang, B. 2013, *ApJ*, 763, L22

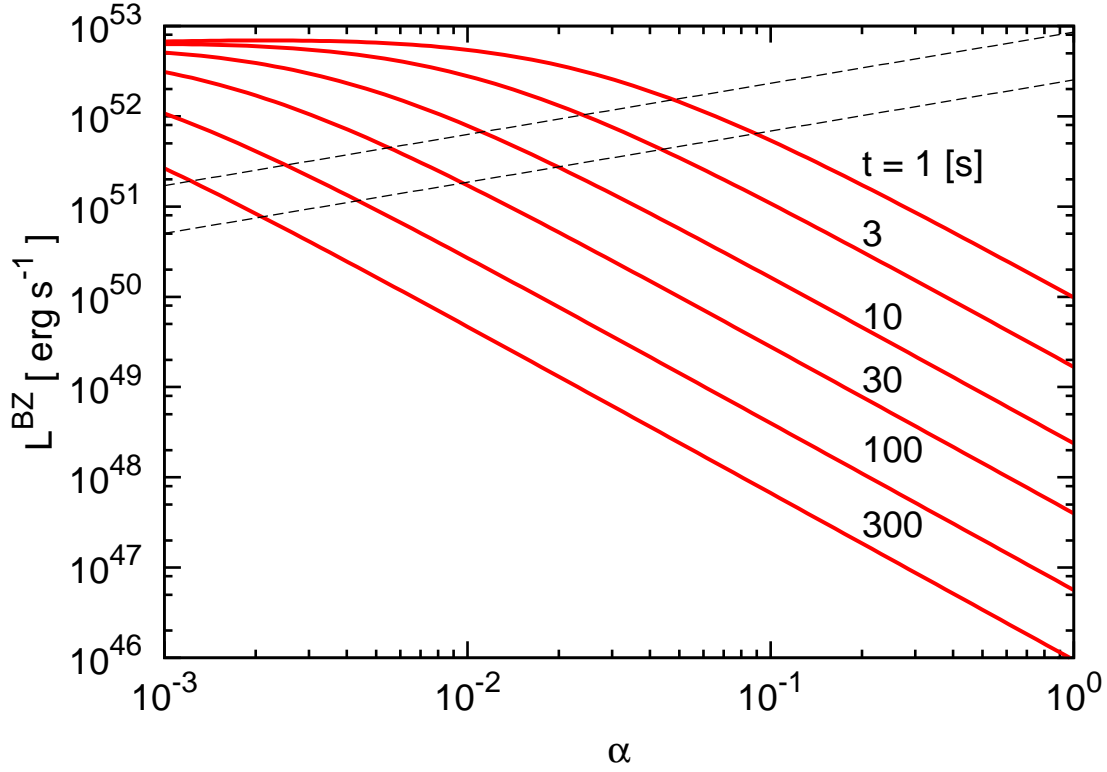


**Figure 2.** The Blandford-Znajek (BZ) luminosity as a function of  $\alpha$  for typical time such as 1 s, 3 s, 10 s, 30 s, 100 s and 300 s for  $m_d^0 = 0.1 M_\odot$ ,  $\beta_0 = 2$ ,  $M_{BH} = 3 M_\odot$ , and  $q = 0.5$ . The magnetic field at the horizon is assumed to be determined by  $B^2 = 8\pi p_{ISCO}$  where  $p_{ISCO}$  is the pressure of the disk at the ISCO ( $r = 6GM_{BH}/c^2$ ) in Eq. (29). The BZ luminosity is then given by Eq. (10). The dashed lines show the neutrino cooling ignition accretion rates for  $q = 0$  (upper) and  $q = 0.95$  (lower).

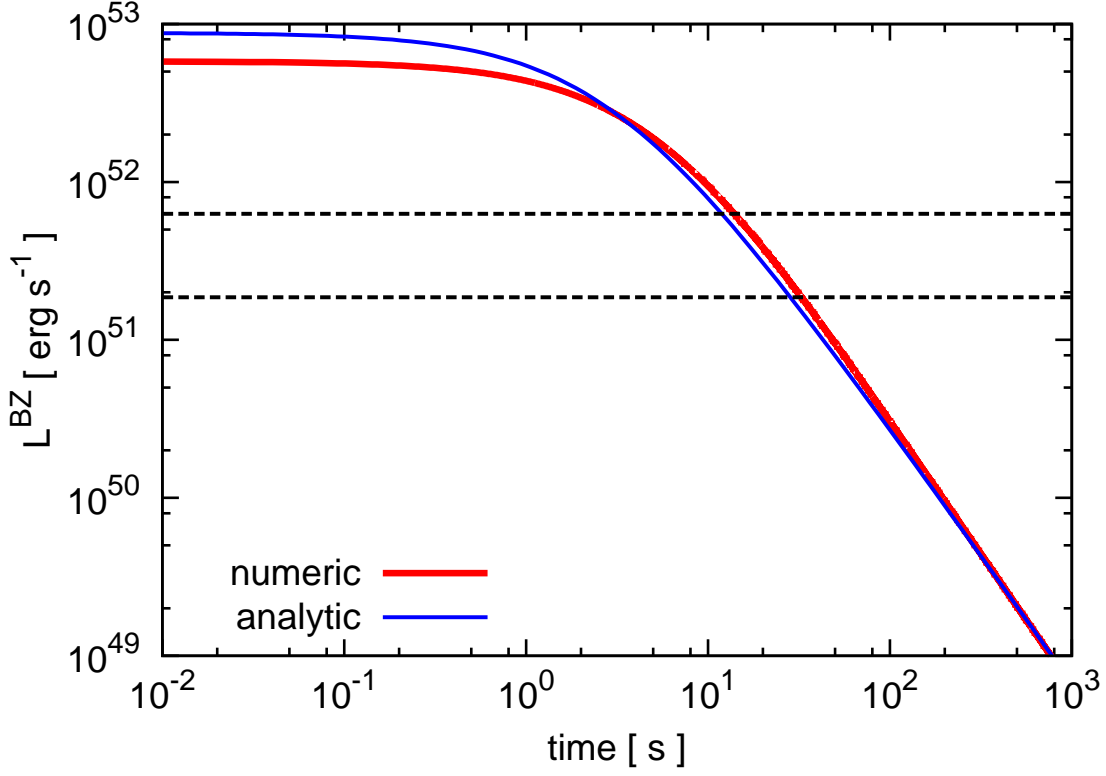


**Figure 3.** Time evolution of the luminosity for  $m_p^0 = 0.1 M_\odot$ ,  $\beta_0 = 2$ ,  $M_{BH} = 3 M_\odot$ ,  $q = 0.5$ , and  $\alpha = 0.01$ . The red and blue solid lines show the numerical exact solution and the analytic approximation, respectively. The dashed lines show the neutrino cooling ignition accretion rates for  $q = 0$  (upper) and  $q = 0.95$  (lower). We see that the analytic approximation only overestimates the luminosity slightly so that we can justify the use of the analytic approximate solution to Eq. (37).

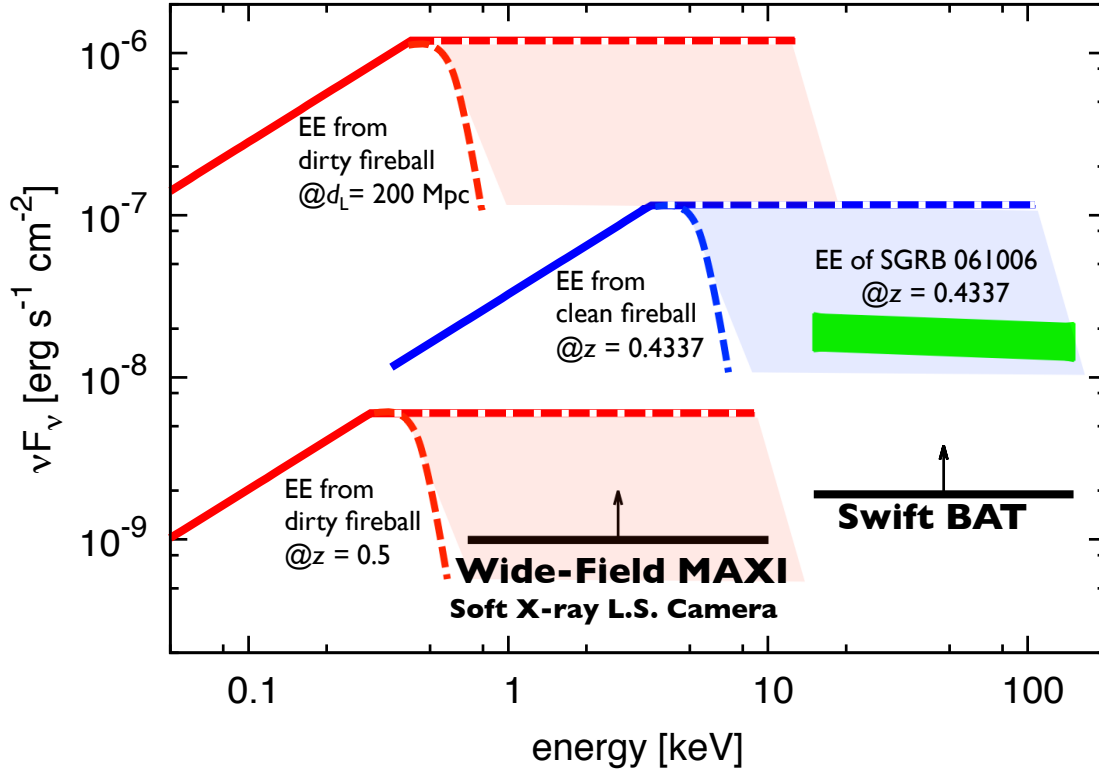


**Figure 4.** Extended emissions (EEs) of short gamma-ray bursts (SGRBs) based on our model and their detectability. The red lines show the anticipated fluxes of the dissipative photospheric emissions from the dirty fireballs (Eqs. 59 and 61) at  $d_L = 200$  Mpc ( $z = 0.046$ ) and  $d_L = 2.8$  Gpc ( $z = 0.5$ ), and the blue line shows the clean fireball case (Eqs. 69 and 70) at  $d_L = 2.4$  Gpc ( $z = 0.4337$ ). The shaded regions represent the uncertainties of the subphotospheric dissipations. If the dissipations are weak, the spectra are quasi-thermal, and if strong, the high energy tails can extend up to  $\varepsilon_{cut} \lesssim 30 \times \varepsilon_{peak}$  with a photo index of  $\lesssim 2$ . The black lines with the upward arrow show the detection thresholds of Wide-Field MAXI (0.7-10 keV) and Swift BAT (15-150 keV). The green thick line shows the observed flux spectrum of the EE associated with SGRB 061006.